COMPONENT SPECIFIC MODELING*

R.L. McKnight and M.T. Tipton
General Electric Company
Aircraft Engine Business Group

INTRODUCTION

The overall objective of this program is to develop and verify a series of interdisciplinary modeling and analysis techniques that have been specialized to address three specific hot section components. These techniques will incorporate data as well as theoretical methods from many diverse areas including cycle and performance analysis, heat transfer analysis, linear and nonlinear stress analysis, and mission analysis. Building on the proven techniques already available in these fields, the new methods developed through this contract will be integrated to provide an accurate, efficient, and unified approach to analyzing combustor burner liners, hollow air-cooled turbine blades, and air-cooled turbine vanes. For these components, the methods developed will predict temperature, deformation, stress, and strain histories throughout a complete flight mission.

The base program for the component specific modeling effort is illustrated in Figure (1). Nine separate tasks have been arranged into two parallel activities. The component specific structural modeling activity in Figure (2), is directed towards the development of the analytical techniques and methodology required in the analysis of complex hot section components. The component specific thermomechanical load mission modeling effort illustrated in Figure (3), provides for the development of approximate numerical models for engine cycle, aerodynamic, and heat transfer analyses of hot section components.

Thermomechanical Load Mission Modeling

In the thermomechanical load mission modeling portion of the program, we developed the Thermodynamic Engine Model (TEM). The TEM is complete and has been developed as a computational tool used to define mission station profiles of gas path engine flow variables and rotor speeds as a function of defined input conditions. Basic input variables for the model are mach number (M), altitude (h) power level (PL). Generated within the model for select aerodynamic stations in the combustor and high pressure gas flowpath are, gas weight flow ($\overset{\bullet}{w}$), temperature (t), pressure (p) and the associated fan (N1) and core (N2) speeds.

The development of the TEM was presented at last years workshop so attention is directed at the capability and accuracy of the model. The accuracy of the model was evaluated relative to the steady state performance computer code (a cycle deck) of a production engine. Noting that the model is based upon multidimensional interpolation of stored data, the maximum error of

---

PRECEDING PAGE BLANK NOT FILMED

```
                    ┌─────────────────┐
                    │    Task I -     │
                    │    Survey       │
                    └────────┬────────┘
                             │
        ┌────────────────────┼────────────────────┐
        ▼                    ▼                     ▼
┌─────────────────┐ ┌─────────────────┐ ┌─────────────────────┐
│   Component-    │ │    Software     │ │    Component-       │
│    Specific    │ │  Development    │ │     Specific        │
│   Structural   │ │                 │ │  Thermomechanical   │
│    Modeling    │ │   ─────────     │ │   Load Mission      │
│                │ │                 │ │     Modeling        │
│   ─────────    │ │    Task IV      │ │                     │
│                │ └─────────────────┘ │   ─────────         │
│   Task II      │                     │                     │
│   Task VI      │                     │   Task III          │
│   Task VIII    │                     │   Task V            │
└───────┬────────┘                     │   Task VII          │
        │                              └──────────┬──────────┘
        └──────────────────┬──────────────────────┘
                           ▼
                  ┌─────────────────┐
                  │   Reporting     │
                  │   Task IX       │
                  └─────────────────┘
```
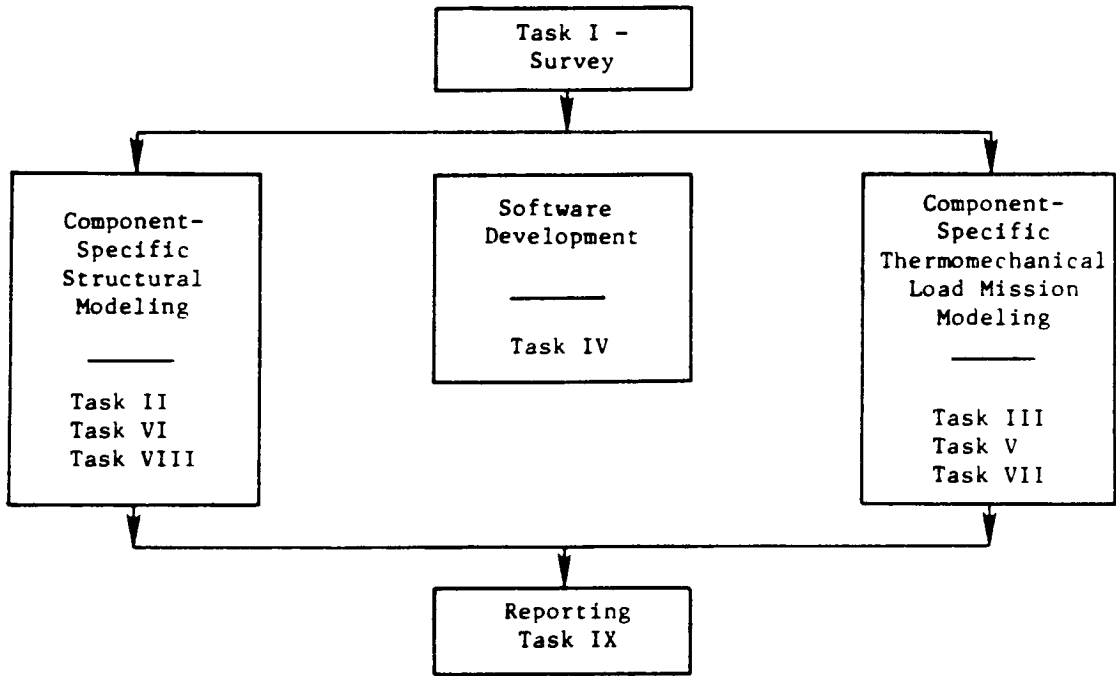
Figure 1. Component Specific Modeling Base Program.

```
┌─────────────────┐                          ┌─────────────────┐
│  Task III       │                          │  Task V         │
│                 │                          │                 │
│  Thermodynamic  │                          │  Mission Model  │
│  Engine Model   │                          │  Decomposition  │
└────────┬────────┘                          └────────┬────────┘
         │                                            │
         │      ┌─────────────────────────────┐       │
         │      │         Task VII            │       │
         │      │                             │       │
         │      │   Thermomechanical Load     │       │
         └─────▶│       Mission Model         │       │
                │       Development           │       │
                │ ─ ─ ─ ─ ─ ─ ─ ─ ─ ─ ─ ─ ─ ─ │       │
                │                             │◀──────┘
                │  Decomposition/Synthesis    │
                │       Capability            │
                │ ─ ─ ─ ─ ─ ─ ─ ─ ─ ─ ─ ─ ─ ─ │
                │                             │
                │       Verification          │
                └─────────────────────────────┘
```
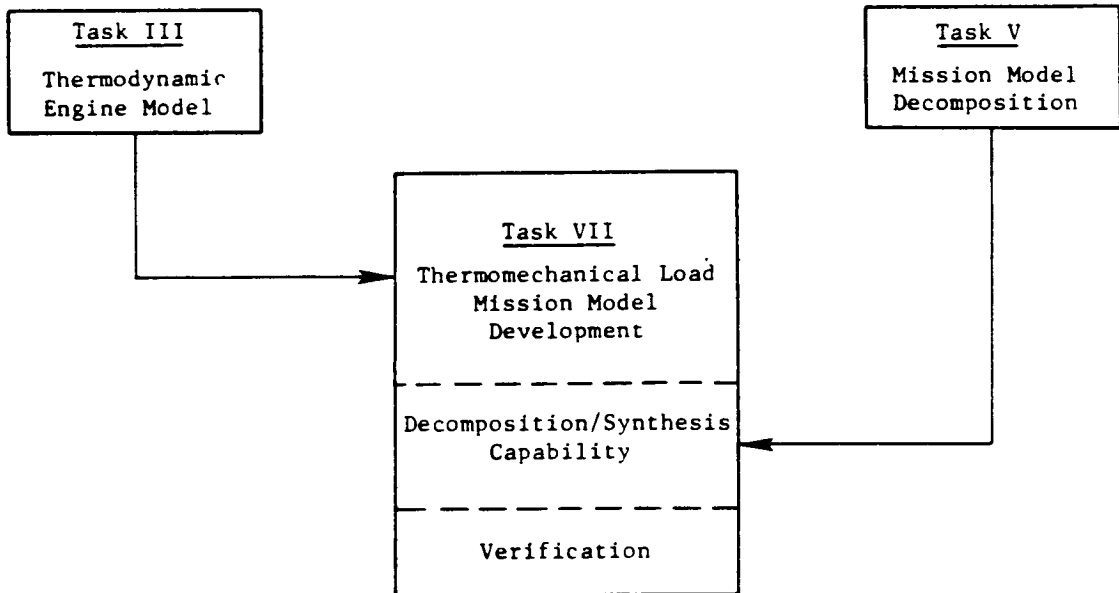
**Figure 2. Component Specific Thermomechanical Load
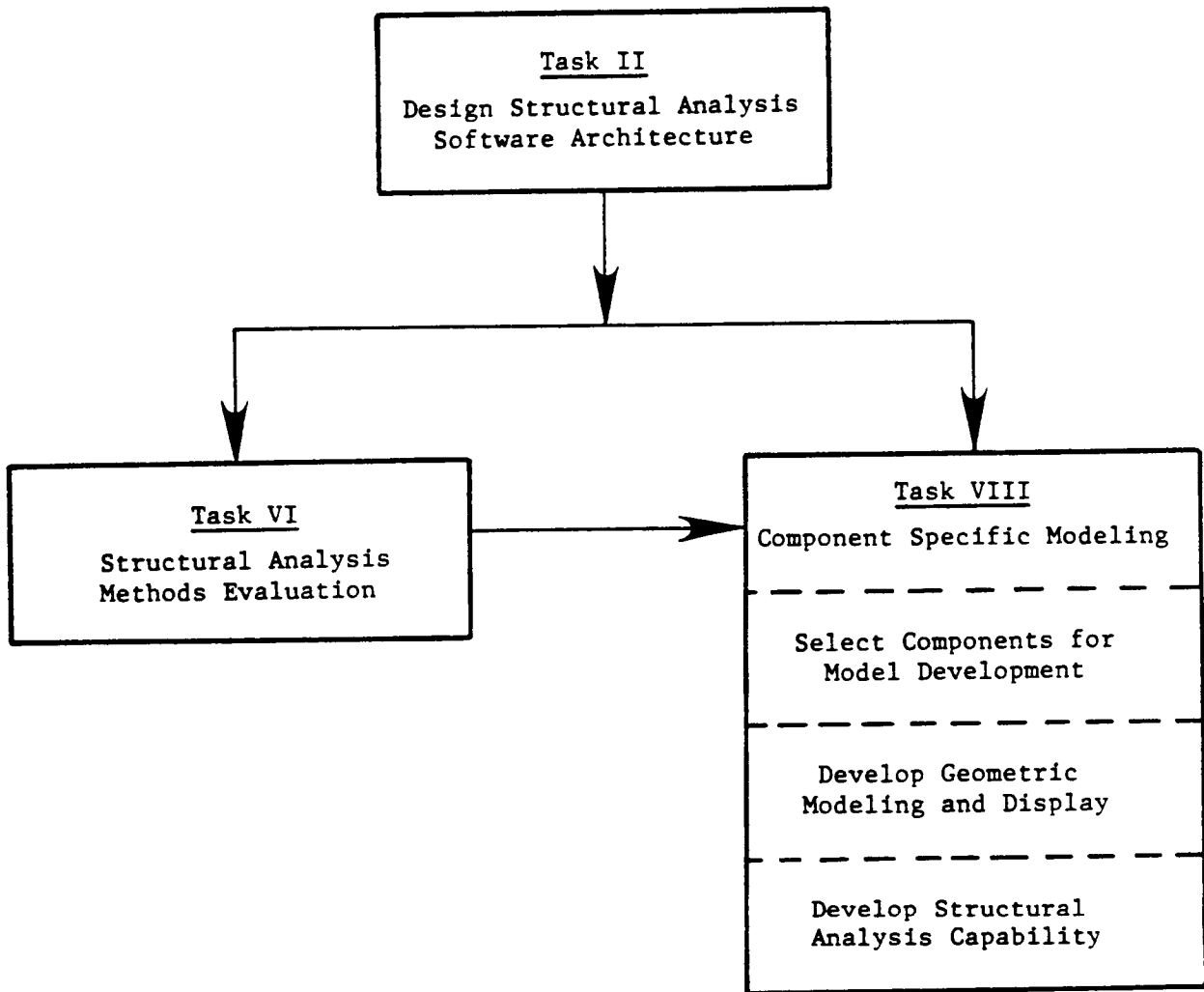   Mission Modeling.**

Figure 3. Component Specific Structural Modeling.

the model should occur at a position the greatest distance from known data points. Illustrated in Figure (4) is an example of a situation in which a region is bounded by four data points with the test point at its center. The region is then subdivided into four rectangles each possessing its own interpolation logic and associated error. Error curves imposed on such a figure illustrate two facts:

(1) The error surface is approximately parabolic and attains its maximum value at the center of the region.

(2) Each quadrant has its own error surface and discontinuities occur where they meet.

Table 1 shows a brief summary of the accuracy level achieved for the TEM. Column 2 shows the average of all test point errors. Columns 3, 4, and 5 show the value that is exceeded 2, 4 and 11 times (1%, 2%, and 5% of the 220 error values). Note that all data in this figure refers to the worst-case test points. Since the error surfaces are approximately parabolic in shape, the average error in each quadrant is approximately half of the maximum error, and the overall error is approximately half of the average error listed.

Table 1 Validation Case Error Analysis

| | | Error Exceeded N Times | | |
	Average	N = 2	N = 4	N = 11
P_2	0.03%	1%	1%	1%
P_3	0.23%	1.3%	1.2%	1.0%
FNIN1	0.49%	1.8%	1.8%	1.8%
XN25	0.17%	0.7%	0.6%	0.5%
T_2	0.08%	5°	5°	5°
T_3	2.1°	10°	10°	10°
T_{41}	11°	47°	47°	35°

Component Specific Structural Modeling

The concepts and techniques developed in the NASA supported ESMOSS program have provided the basis to create an efficient modeling system for specific hot section engine components. The modeling and subsequent discretization of model geometries is component dependent and follows either a recipe or a data point/curve fit format. The capability to create geometric and discretized models of these components is well under development and examples of such are illustrated in Figure (5).

Finite Element Methods

This phase of the program centers on the development, implementation and evaluation of both new and existing analytical methods for the non-linear stress analysis of select hot section components. Within the structural
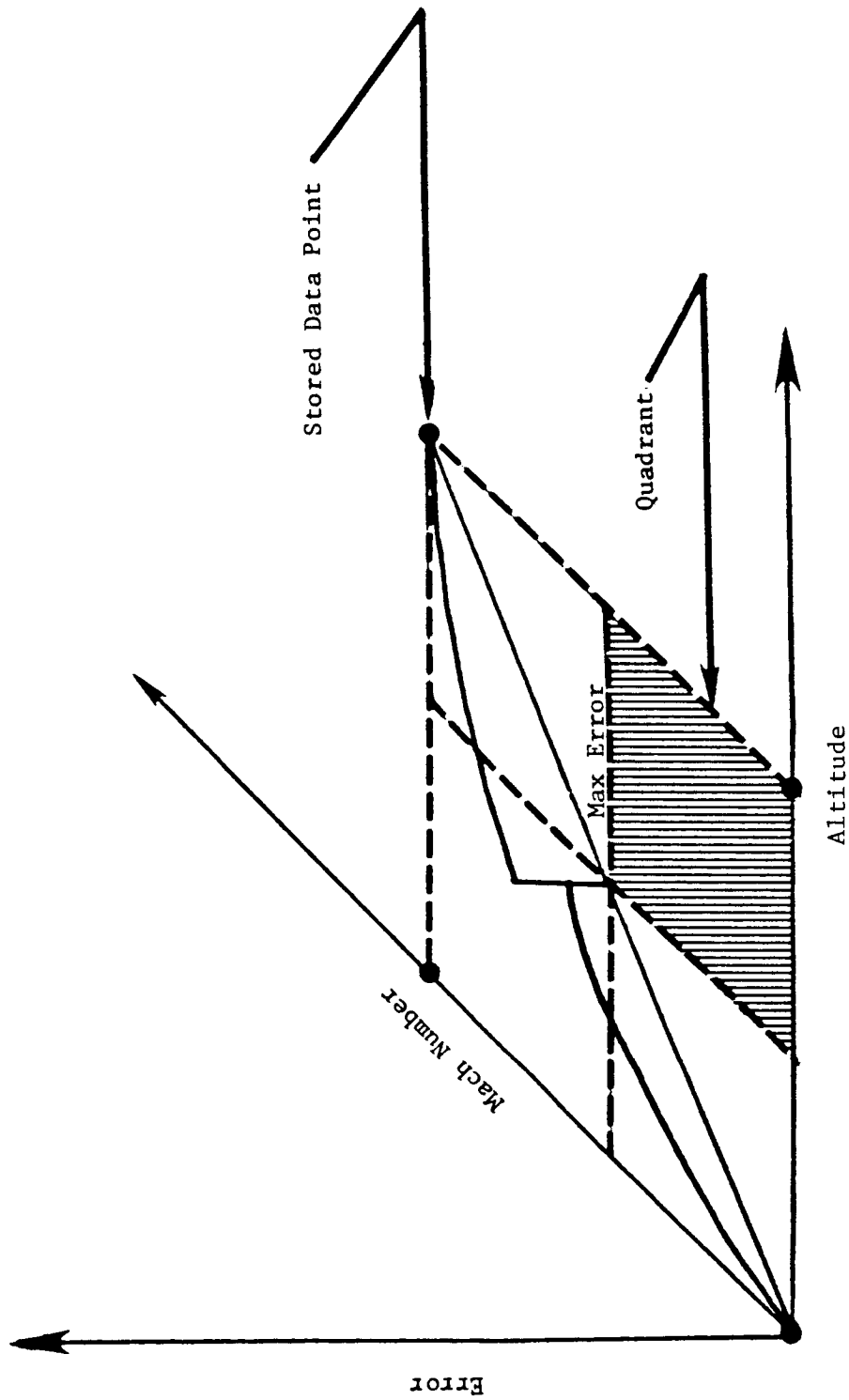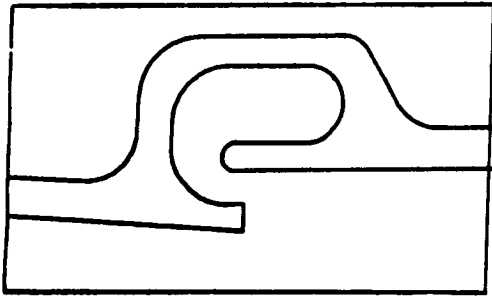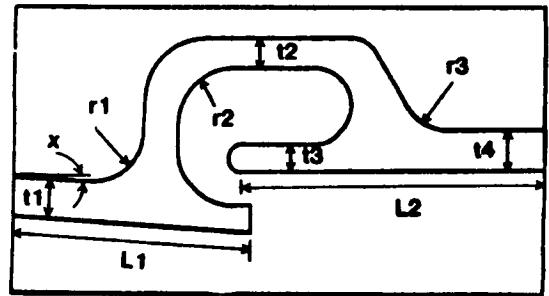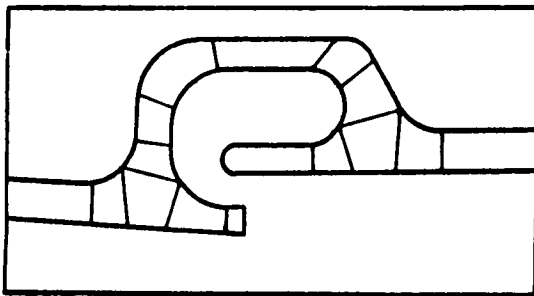
Stored Data Point

Quadrant.

Max Error

Mach Number

Error

Altitude
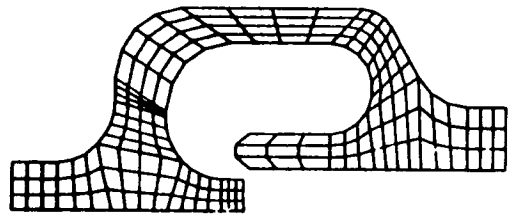
Figure 4. Quadrant Error Distribution.
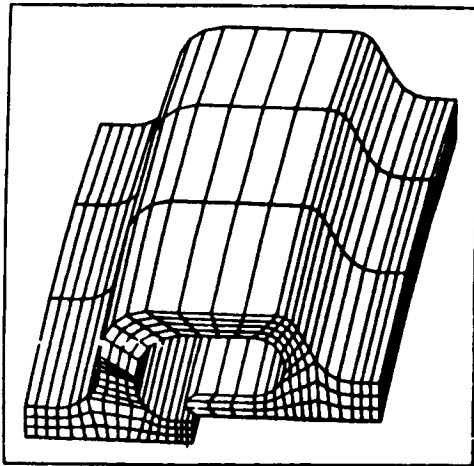
249

Typical Nugget

Physical Input Parameters
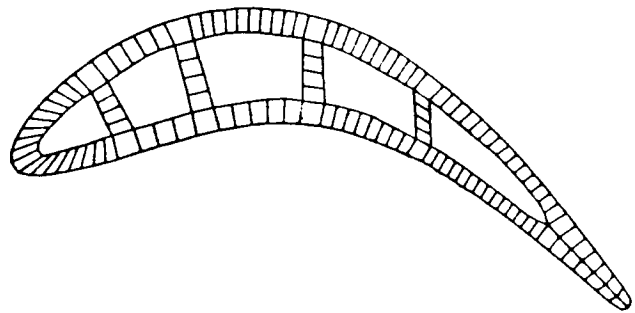
Master Region Definition

2D Model

3D Model

Turbine Blade with Cavities

Figure 5. Examples of Component Specific Structural Modeling Capabilities.

250

analysis software exist several new and innovative concepts. Embedded in the code are several classical solution algorithms, three constitutive models, "self-adaptive" type solution techniques, and the capability for remeshing and mesh refinement.

As noted, several classical solution techniques have been included in the code. It is intended that such a selection of solution algorithms will afford the user (and the programmer) a choice as to method of solution as well as to provide for adaptability of the code to problem definition and machine residency. Solution algorithms currently include:

(A) SESOL

- A sparse matrix solver with a skyline storage scheme.

(B) COLSOL

- A vectorized column solver.

(C) Frontal Method

- Currently under development.

In addition to our library of select solution techniques, we have included in our analysis code an alternate method for defining convergence of the numerical solution. Our current work has focused upon vector norms due to their structure, computational simplicity and potential applicability to self-adaptive solution strategies and techniques. Vector norms provide the means by which both quantitative and qualitative statements can be made between associated vectors. Noting that our current solution scheme is an iterative technique, we are looking at the convergence of a series of vectors (i.e. displacements). In such an application it is necessary to determine when a solution has been obtained as well as to determine the quality of that solution.

Convergence of the numerical solution can be determined on either the local or global level. Currently within our code we use a local or point-by-point method and the present work represents an effort to see if a global scheme has applicability.

There can be defined infinitely many norms but the three most common norms are the ℓ_p norms, $||\cdot||_p$ for $P = 1$, 2, and ∞.

$$||\cdot||_1 = |\bar{x}_1| + |\bar{x}_2| + |\bar{x}_3| + \ldots\ldots |\bar{x}_N|$$

$$||\cdot||_2 = \left[|\bar{x}_1|^2 + |\bar{x}_2|^2 + |\bar{x}_3|^2 + \ldots\ldots |\bar{x}_N|^2 \right]^{1/2}$$

$$||\cdot||_\infty = \max \left\{ |\bar{x}_1|, |\bar{x}_2|, |\bar{x}_3|, \ldots\ldots |\bar{x}_N| \right\}$$

The above norms are special cases of the vector norm:

$$\left(\sum_{i=1}^{N} (\bar{x}_i)^P \right)^{1/P}$$

To utilize the norms defined above the concept of relative and absolute error can be defined (1) for any two vectors, the absolute error can be written as:

$$E^A = \|\bar{x}_i\| - \|\bar{x}_{i-1}\|$$

And the relative error written as:

$$E^R = \frac{\|\bar{x}_i\| - \|\bar{x}_{i-1}\|}{\|\bar{x}_{i-1}\|}$$

The expression for relative error tends to be far more applicable to our needs and its structure lends itself conveniently to the formulation of convergence criteria in iterative methods. Convergence can be assumed when the magnitude of a norm, or the difference between norms of successive iterations is less than some predefined tolerance. From the above, six separate norms were defined, and then included in the code for evaluation.

1. $$\frac{\|\bar{x}_i\|_1 - \|\bar{x}_{i-1}\|_1}{\|\bar{x}_{i-1}\|_1}$$ 2. $$\frac{\|\bar{x}_i\|_1 - \|\bar{x}_{i-1}\|_1}{\|\bar{x}_i\|_1}$$

3. $$\frac{\|\bar{x}_i\|_2 - \|\bar{x}_{i-1}\|_2}{\|\bar{x}_{i-1}\|_2}$$ 4. $$\frac{\|\bar{x}_i\|_2 - \|\bar{x}_{i-1}\|_2}{\|\bar{x}_i\|_2}$$

5. $$\frac{\|\bar{x}_i\|_\infty - \|\bar{x}_{i-1}\|_\infty}{\|\bar{x}_{i-1}\|_\infty}$$ 6. $$\frac{\|\bar{x}_i\|_\infty - \|\bar{x}_{i-1}\|_\infty}{\|\bar{x}_i\|_\infty}$$

To provide the user with a choice and offer some versatility in the modeling of non-linear material behavior, three separate material constitutive

models have been coded into the analysis program. These constitutive models are:

(A) Haisler-Allen model

(B) Bodner's Model

(C) A Simplified Model

We are using remeshing and mesh refinement techniques in our self-adaptive solution strategies. Work is focused on the examination of methods and techniques required to upgrade the mesh and criteria by which this process is activated. Methods of mesh refinement could include progressive subdivision, mesh realignment and upgrade of element order. Criteria for mesh refinement may include strain energy density, elemental stress/strain gradients, inter-element stress/strain gradients and nodal stress comparisons. We are currently in the evaluation phase of the above and our strategy for proceeding in this area involves the following:

(a) Select an analytical model with known solutions.

(b) Analyze several meshes of different density.

(c) Use the 20 noded brick element to evaluate remeshing criteria.

For our initial work we have selected a semi-infinite plate with a circular hole near the edge. Figure (6) shows the recipe parameters and master region definition for the problem and Figure (7) illustrates the coarse, medium and refined meshes for such a model.

For a 2D plane stress conditions, the models were fixed at the left edge and subjected to a uniform tensile stress at the right edge. Comparisons were then made as to the adequacy of computed surface stresses and inter-element stress distributions. A summary of the above appear in Figures (8) and (9).

CONCLUSIONS

When complete, this program will provide the engineer with a total non-linear stress analysis system designed for hot section component parts. The system will enable the engineer to address the effects of mission variation and design changes on component response while demonstrating efficiency and versatility in application. The system will provide new and innovative technology in the area of non-linear high temperature stress analysis and in turn make a significant contribution to assessing hot section component durability.

Master Region Model
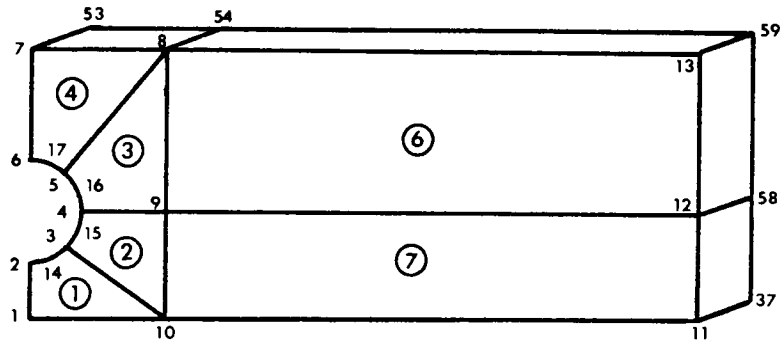
Parameters
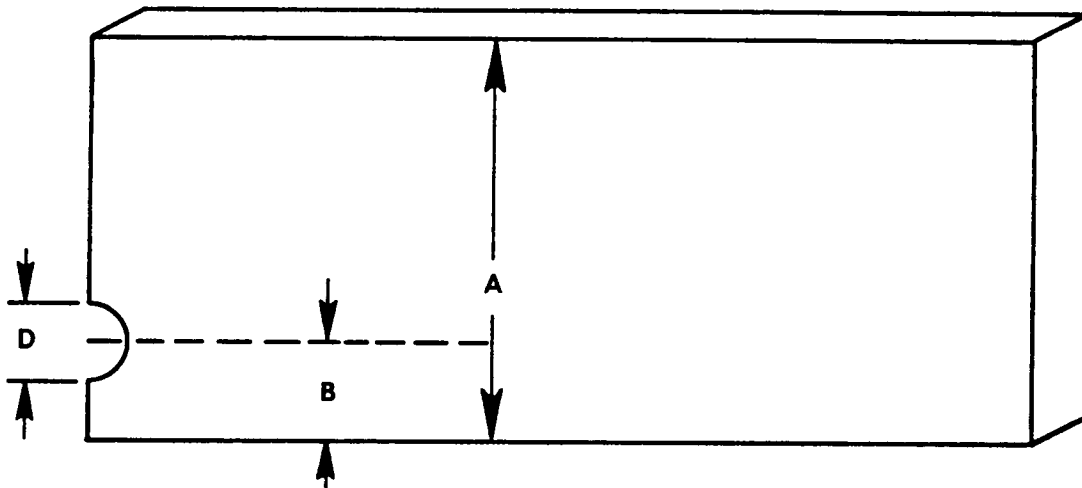
A = Height
B = Relative Placement of Center
    of Hole Relative to A
D = Diameter of Hole

Input: D as a Percentage of the Height
        B as a Percentage of the Height

Note: The Hole Cannot be Placed Beyond the
       Limits of the Beam

(Ex) Input = 20%, 23.334%
     Set a 0.2A Hole
         0.2334 A Center

Figure 6. Recipe Parameters and Master Region Model for Plate
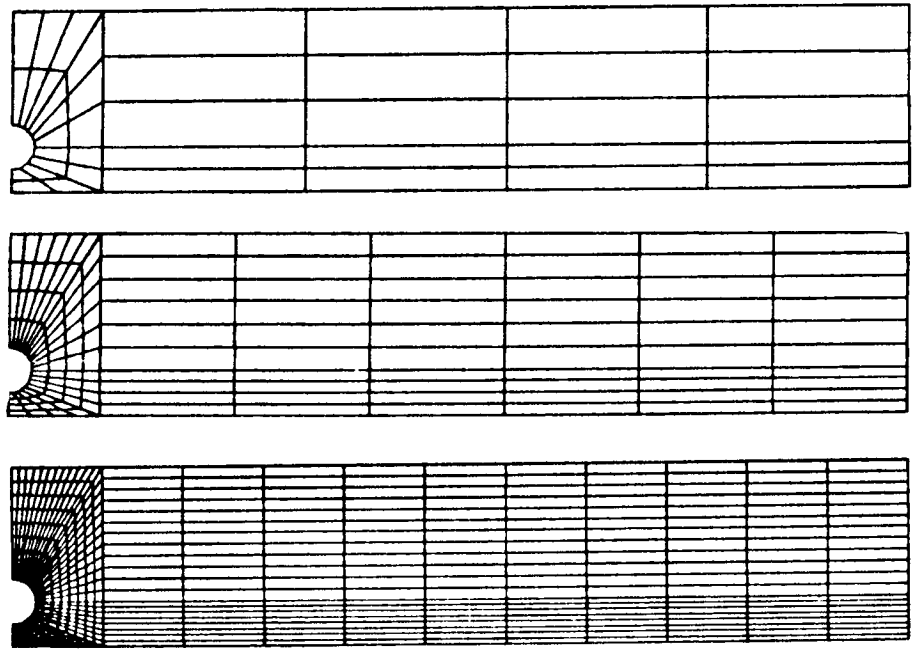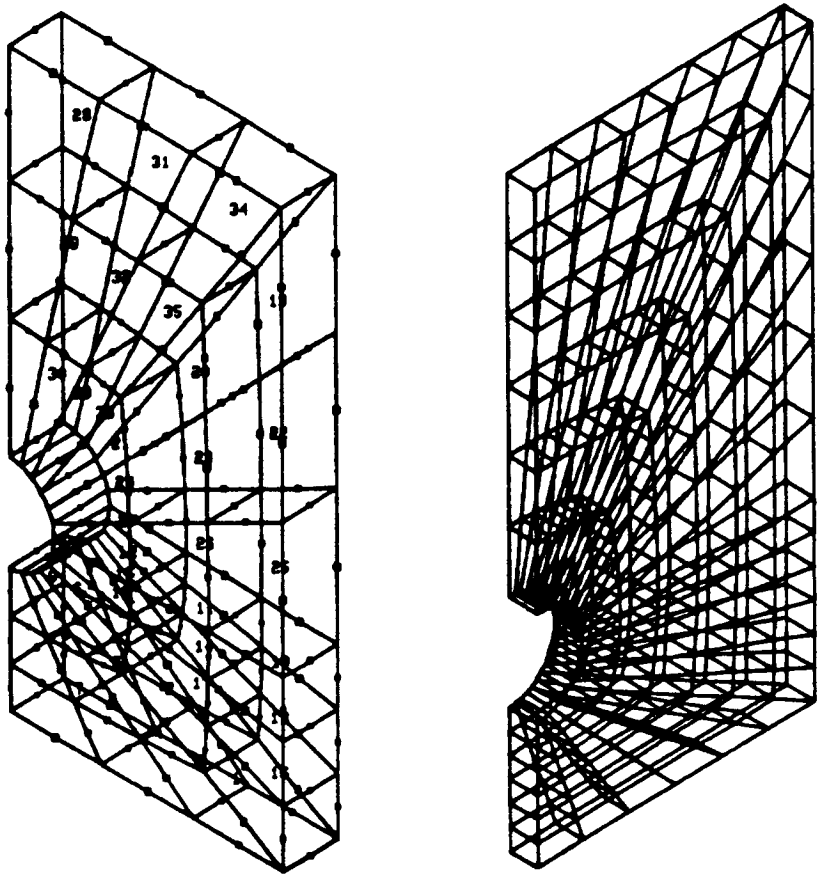   with Hole.

254

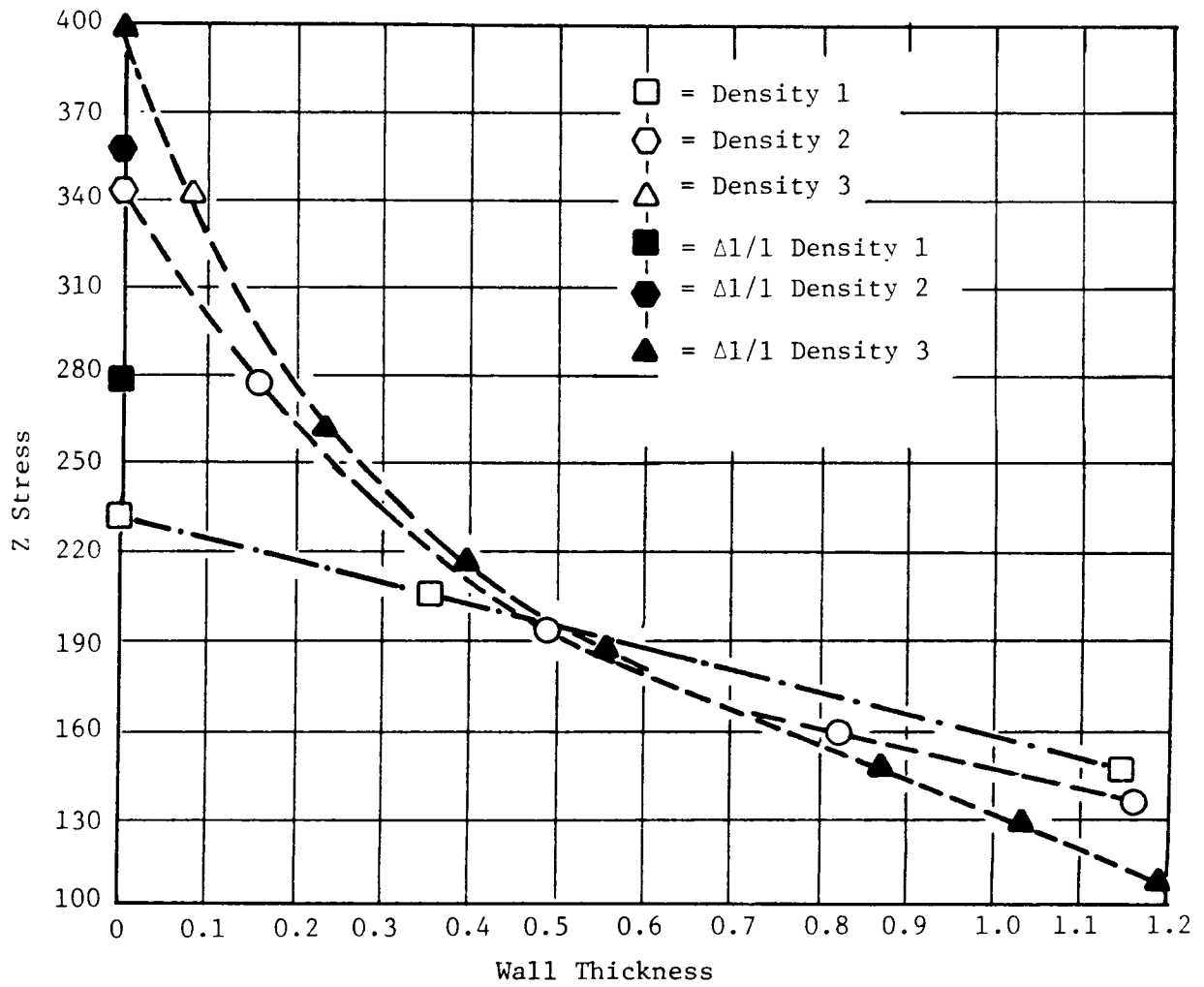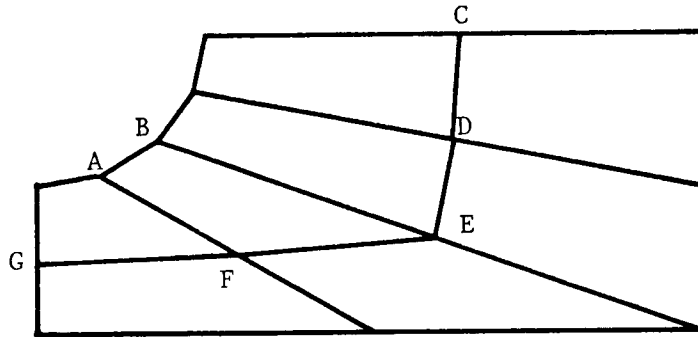Figure 7. Discretized Mesh Geometries for Semi-Infinite Plate Model.

Figure 8. Effect of Mesh Density on Stress Prediction.

C

B

A

D

G

F

E

Points In Model	MESH (Figure 33)							
	1		2		3		4	
	σ_{Max} Diff ksi	$\frac{\sigma_{Max} \, Diff}{\sigma_{Avg}}$ x100	σ_{Max} Diff ksi	$\frac{\sigma_{Max} \, Diff}{\sigma_{Avg}}$ x100	σ_{Max} Diff ksi	$\frac{\sigma_{Max} \, Diff}{\sigma_{Avg}}$ x100	σ_{Max} Diff ksi	$\frac{\sigma_{Max} \, Diff}{\sigma_{Avg}}$ x100
A	71	42	58	30	42	20	34	15
B	46	42	38	37	26	30	20	35
C	29	38	19	26	11	15	8	11
D	46	53	28	33	16	19	11	13
E	46	41	18	16	11	9	8	7
F	83	55	29	20	12	8	7	4
G	58	33	34	20	22	12	16	9

Figure 9.   Results of the Effect of Mesh Density.

257